Journal of Systems Engineering and Electronics
Vol. 32, No. 2, April 2021, pp.487 – 497

A robust subband adaptive filter algorithm for sparse and block-sparse systems identification

ZAHRA Habibi[1,*], HADI Zayyani[2], and MOHAMMAD Shams Esfand Abadi[3]

1. Research Institute for Information and Communications Technologies, Academic Center for Education, Culture and Research, Tehran 1599616313, Iran; 2. Department of Electrical and Computer Engineering, Qom University of Technology, Qom 371951519, Iran; 3. Faculty of Electrical Engineering, Shahid Rajaee Teacher Training University, Tehran 1678815811, Iran

Abstract: This paper presents a new subband adaptive filter (SAF) algorithm for system identification scenario under impulsive interference, named generalized continuous mixed p-norm SAF (GCMPN-SAF) algorithm. The proposed algorithm uses a GCMPN cost function to combat the impul- sive interference. To further accelerate the convergence rate in the sparse and the block-sparse system identification processes, the proportionate versions of the proposed algorithm, the L_0-norm GCMPN-SAF (L_0-GCMPN-SAF) and the block-sparse GCMPN-SAF (BS-GCMPN-SAF) algorithms are also developed. Moreover, the convergence analysis of the proposed algorithm is provided. Simulation results show that the proposed algorithms have a better performance than some other state-of-the-art algorithms in the literature with respect to the convergence rate and the tracking capability.

Keywords: subband adaptive filter (SAF), generalized continuous mixed p-norm (GCMPN), sparse system, block-sparse system, impulsive interference.

DOI: 10.23919/JSEE.2021.000041

1. Introduction

The least-mean-square (LMS) and the normalized LMS (NLMS) adaptive filtering algorithms have been widely used in various applications such as system identification, channel equalization and noise cancellation [1]. However, unfortunately, the mentioned algorithms converge slowly when their input signal is colored.

To further speed up the convergence rate of an adaptive filter for colored input signals, in subband adaptive filter (SAF), the colored input signals are divided into multiple approximately white subband signals [2]. In [3], the normalized SAF (NSAF) algorithm has approximately the same complexity as the NLMS algorithm, while its convergence rate is higher. In many system identification scenarios, for example, acoustic echo path, the system impulse response is sparse or block-sparse [4−6]. It is noteworthy that in the sparse system, most coefficients are zero or near zero and just a few of them are nonzero, and in the block-sparse system, the coefficients are in the form of a single cluster or multi-cluster, where in a cluster is a gathering of the nonzero coefficients. In comparison to the NSAF algorithm, the proportionate NSAF (PNSAF) algorithm has a fast initial convergence, when the echo path is sparse. However, unfortunately, this algorithm has a slow convergence after the initial fast convergence, and a poor performance for the dispersive systems [7]. The improved PNSAF (IPNSAF) has a good performance for both the sparse and the dispersive systems [7]. To keep the fast initial convergence speed during the whole adaptation process until the adaptive filter reaches its steady state, the μ-law PNSAF (MPNSAF) has been proposed in [7]. However, these algorithms are not robust against impulsive interference.

Recently, several subband adaptive filter algorithms have been proposed in [8−17], which show a good robustness against impulsive interference. In [8], the sign subband adaptive filter (SSAF) algorithm, by using the idea that lower order statistics can improve robustness against impulsive interference, minimized an L_1-norm of the subband a posteriori error vector of the filter. To enhance the performance of the SSAF algorithm, several algorithms have been developed in [9−17]. The individual-weighting-factor SSAF (IWF-SSAF) algorithm in [16] used an IWF for each subband. Moreover, in [17], the normalized logarithmic SAF (NLSAF) algorithm has the same convergence rate as the SSAF with less steady state error.

To speed up the convergence rate in the sparse system identification scenario, several SAF algorithms have been proposed in [7,18−23]. The proportionate SSAF (P-SSAF)

Manuscript received March 24, 2020.
*Corresponding author.

algorithm and the affine projection SSAF (AP-SSAF) algorithms have been presented in [21]. The L_0-norm SSAF (L_0-SSAF) and the L_0-norm NLSAF (L_0-NLSAF) algorithms in [22,23] have been derived by inserting a penalty of sparsity, i.e., L_0-norm of the adaptive tap-weights, into the SSAF and the NLSAF algorithms cost functions, respectively. In addition, the developed algorithm named individual-weighting-factor improved PSSAF (IWF-IPSSAF) has been proposed in [17]. Recently, several algorithms have been proposed for the block-sparse system identification scenario [24−29]. In the block-sparse LMS (BS-LMS) algorithm [24], a penalty of block-sparsity, which is a mixed $L_{2,0}$-norm of the adaptive tap-weights with the equal group partition sizes inserted into the cost function of the conventional LMS algorithm.

The generalized variable step size continuous mixed p-norm (GVSS-CMPN) algorithm in [30] demonstrates a good robustness against impulsive interference by minimizing the p-norms of the system output error, where p is a continuous value from 1 to 2. However, according to the simulations, it has a slow convergence rate for the colored input signal. In order to solve this problem, we present a new SAF algorithm named generalized continuous mixed p-norm SAF (GCMPN-SAF) with its convergence analysis, in this paper. To further speed up the convergence rate, for the sparse and the block-sparse systems identification processes, a family of the proposed algorithms are also proposed. In general, our main contributions are as follows:

(i) In order to speed up the convergence rate of the robust GVSS-CMPN algorithm, for the colored input signals, we apply the SAF-structure to this algorithm. According to the simulation results, we can see that the proposed algorithm has a good robustness against impulsive interference, and also exhibits a proper convergence rate and tracking capability for the colored input signals. Also, the proposed algorithms have a better performance than some other state-of-the-art algorithms in the literature with respect to the convergence rate and the tracking capability.

(ii) In order to improve the performance of the proposed algorithm for the sparse and the block-sparse systems identification processes, the proportionate versions of the GCMPN-SAF algorithm, named proportionate GCMPN-SAF (PGCMPN-SAF), improved PGCMPN-SAF (IPGCMPN-SAF), and μ-law PGCMPN-SAF (MPGCMPN-SAF) algorithms are developed. Also, for a better sparse system identification, we propose another algorithm L_0-GCMPN-SAF which is derived by inserting an L_0-norm of the adaptive tap-weights into the GCMPN-SAF algorithm cost function. In order to improve the performance of the proposed algorithm, for the block-sparse system identification process, we also develop the BS-GCMPN-SAF algorithm which is derived by inserting a mixed $L_{2,0}$-norm of the adaptive tap-weights with the equal group partition sizes to the GCMPN-SAF algorithm cost function. Simulation results show that the proportionate versions of the proposed algorithm have a better performance than the non-proportionate counterparts GCMPN-SAF, L_0-GCMPN-SAF and BS-GCMPN-SAF algorithms for both the sparse and the block-sparse systems. Similar to [7], we can see that the MPGCMPN-SAF algorithm has a better performance than the IP-GCMPN-SAF algorithm, and the IPGCMPN-SAF algorithm has a better performance than the PGCMPN-SAF algorithm. Also, the performance of the BS-GCMPN-SAF algorithm is better than the L_0-GCMPN-SAF algorithm, especially for the block-sparse system.

2. Review of the SAF algorithm

In the system identification process, the desired signal $d(n)$ is obtained as

$$d(n) = \boldsymbol{u}^{\mathrm{T}}(n)\boldsymbol{w}_{\mathrm{o}} + \eta(n) \tag{1}$$

where $\boldsymbol{u}(n) = [u(n), u(n-1), \cdots, u(n-M+1)]^{\mathrm{T}}$ is the input signal vector, $\boldsymbol{w}_{\mathrm{o}}$ denotes the unknown weight vector with the length M and $\eta(n)$ is the additive noise which includes the white Gaussian background noise $\nu(n)$ and the impulsive interference $\chi(n)$. Fig. 1 shows the structure of the SAF with N subbands. The analysis filters $\{H_0(z), H_1(z), \cdots, H_{N-1}(z)\}$ partition the input signal $\boldsymbol{u}(n)$ and desired signal $d(n)$ into N subband signals $\boldsymbol{u}_i(n)$ and $d_i(n)$ respectively. The subband signals $y_i(n)$ are the output of the adaptive filter whose weight vector is represented as $\boldsymbol{w}(k) = [w_0(k), w_1(k), \cdots, w_{M-1}(k)]^{\mathrm{T}}$. The signals $y_{i,D}(k)$ and $d_{i,D}(k)$ are generated by N-fold decimation of the signals $y_i(n)$ and $d_i(n)$, respectively. It is easy to obtain that

$$d_{i,D}(k) = \boldsymbol{u}_i^{\mathrm{T}}(k)\boldsymbol{w}_{\mathrm{o}} + \eta_i(k) \tag{2}$$

and

$$y_{i,D}(k) = \boldsymbol{u}_i^{\mathrm{T}}(k)\boldsymbol{w}(k) \tag{3}$$

where $d_{i,D}(k) = d_i(kN)$, $\boldsymbol{u}_i(k) = [u_i(kN), u_i(kN-1), \cdots, u_i(kN-M+1)]^{\mathrm{T}}$ and $\eta_i(k)$ is the ith subband noise. Also, the subband error signals $e_{i,D}(k)$ for $i = 0, 1, \cdots, N-1$ are obtained as

$$e_{i,D}(k) = d_{i,D}(k) - y_{i,D}(k) = d_{i,D}(k) - \boldsymbol{u}_i^{\mathrm{T}}(k)\boldsymbol{w}(k). \tag{4}$$

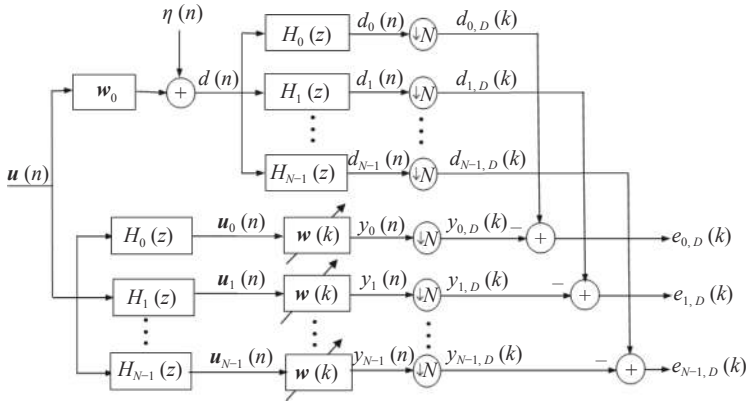

Fig. 1 Structure of the SAF

3. The proposed algorithm

In order to speed up the convergence rate of the robust GVSS-CMPN algorithm [30] for the colored input signal, this paper introduces a new SAF algorithm named GCMPN-SAF algorithm, which benefits from the following GVSS-CMPN cost function [30]:

$$J(k)=\int_1^2 \lambda(p)\mathrm{E}\{|\boldsymbol{e}_D(k)|^p\}\mathrm{d}p \tag{5}$$

where $\lambda(p)=\theta\left(p-\frac{3}{2}\right)+1$ denotes the weighting factor, θ is a regulating factor in the interval $[-2,2]$, $e_D(k)=[e_{0,D}(k),\cdots,e_{N-1,D}(k)]^{\mathrm{T}}$ and $\mathrm{E}\{\cdot\}$ denotes the expectation [30]. Here, according to (5) and the SAF structure in [2], the proposed cost function is detailed as

$$J(k)=\sum_{i=0}^{\mathrm{N}-1}\int_1^2 \lambda(p)\mathrm{E}\left\{\left|e_{i,D}(k)\right|^p\right\}\mathrm{d}p. \tag{6}$$

By using the steepest descent principle, we have

$$\boldsymbol{w}(k+1)=\boldsymbol{w}(k)-\mu\nabla_{\boldsymbol{w}(k)}J(k) \tag{7}$$

where μ denotes the fixed step size ($\mu>0$), and $\nabla_{\boldsymbol{w}(k)}$ from (6) is given by

$$\nabla_{\boldsymbol{w}(k)}J(k)=\sum_{i=0}^{N-1}\int_1^2 \lambda(p)\frac{\partial}{\partial\boldsymbol{w}(k)}\mathrm{E}\left\{\left|e_{i,D}(k)\right|^p\right\}\mathrm{d}p. \tag{8}$$

By using the $|e_{i,D}(k)|^p$ instead of the $\mathrm{E}\{|e_{i,D}(k)|^p\}$, and substituting (4) into (8), we get

$$\nabla_{\boldsymbol{w}(k)}J(k)=$$
$$\sum_{i=0}^{N-1}\boldsymbol{u}_i(k)\mathrm{sign}(e_{i,D}(k))\int_1^2 p\lambda(p)\left|e_{i,D}(k)\right|^{p-1}\mathrm{d}p \tag{9}$$

where sign(·) denotes the sign function.

Therefore, we can rewritten (7) as

$$\boldsymbol{w}(k+1)=\boldsymbol{w}(k)+\mu\sum_{i=1}^{N-1}\varepsilon_i(k)\boldsymbol{u}_i(k)\mathrm{sign}(e_{i,D}(k)) \tag{10}$$

where

$$\varepsilon_i(k)=\int_1^2 p\lambda(p)|e_{i,D}(k)|^{p-1}\mathrm{d}p. \tag{11}$$

We consider the weighting factor $\lambda(p)$ in (11) as

$$\lambda(p)=\frac{\theta\left(p-\frac{3}{2}\right)+1}{\sqrt{\sum_{i=0}^{N-1}\boldsymbol{u}_i^{\mathrm{T}}(k)\boldsymbol{u}_i(k)+\gamma}} \tag{12}$$

where θ similar to [29] is a regulating factor in the interval $[-2,2]$, and γ is a small positive value to avoid dividing by zero. Based on (12), (11) can be rewritten as

$$\varepsilon_i(k)=\int_1^2 p\frac{\theta\left(p-\frac{3}{2}\right)+1}{\sqrt{\sum_{i=0}^{N-1}\boldsymbol{u}_i^{\mathrm{T}}(k)\boldsymbol{u}_i(k)+\gamma}}|e_{i,D}(k)|^{p-1}\mathrm{d}p=$$
$$\frac{\int_1^2 p\theta\left(p-\frac{3}{2}\right)|e_{i,D}(k)|^{p-1}\mathrm{d}p+\int_1^2 p|e_{i,D}(k)|^{p-1}\mathrm{d}p}{\sqrt{\sum_{i=0}^{N-1}\boldsymbol{u}_i^{\mathrm{T}}(k)\boldsymbol{u}_i(k)+\gamma}}=$$
$$\theta\delta(k)+\rho(k) \tag{13}$$

where from [29,30] we have

$$\delta(k)\triangleq\frac{\int_1^2 p\left(p-\frac{3}{2}\right)\left|e_{i,D}(k)\right|^{p-1}\mathrm{d}p}{\sqrt{\sum_{i=0}^{N-1}\boldsymbol{u}_i^{\mathrm{T}}(k)\boldsymbol{u}_i(k)+\gamma}}=$$
$$\frac{\frac{2\left|e_{i,D}(k)\right|-2}{\ln^3\left|e_{i,D}(k)\right|}+\frac{0.5-2.5\left|e_{i,D}(k)\right|}{\ln^2\left|e_{i,D}(k)\right|}+\frac{\left|e_{i,D}(k)\right|+0.5}{\ln\left|e_{i,D}(k)\right|}}{\sqrt{\sum_{i=0}^{N-1}\boldsymbol{u}_i^{\mathrm{T}}(k)\boldsymbol{u}_i(k)+\gamma}} \tag{14}$$

and

$$\rho(k) \triangleq \frac{\int_1^2 p\left|e_{i,D}(k)\right|^{p-1}\mathrm{d}p}{\sqrt{\sum_{i=0}^{N-1}\boldsymbol{u}_i^{\mathrm{T}}(k)\boldsymbol{u}_i(k)+\gamma}} = \frac{\dfrac{\ln\left|e_{i,D}(k)\right|\left(2\left|e_{i,D}(k)\right|-1\right)-\left|e_{i,D}(k)\right|+1}{\ln^2\left|e_{i,D}(k)\right|}}{\sqrt{\sum_{i=0}^{N-1}\boldsymbol{u}_i^{\mathrm{T}}(k)\boldsymbol{u}_i(k)+\gamma}}. \tag{15}$$

Therefore, we can summarize (13) as

$$\varepsilon_i(k) = \frac{\alpha_i(k)}{\sqrt{\sum_{i=0}^{N-1}\boldsymbol{u}_i^{\mathrm{T}}(k)\boldsymbol{u}_i(k)+\gamma}} \tag{16}$$

where

$$\alpha_i(k) = \theta\left(\frac{2\left|e_{i,D}(k)\right|-2}{\ln^3\left|e_{i,D}(k)\right|}+\frac{0.5-2.5\left|e_{i,D}(k)\right|}{\ln^2\left|e_{i,D}(k)\right|}+\frac{\left|e_{i,D}(k)\right|+0.5}{\ln\left|e_{i,D}(k)\right|}\right) \frac{\dfrac{\ln\left|e_{i,D}(k)\right|\left(2\left|e_{i,D}(k)\right|-1\right)-\left|e_{i,D}(k)\right|+1}{\ln^2\left|e_{i,D}(k)\right|}}{}. \tag{17}$$

Finally, we can rewrite the update formula for tap-weights of the proposed GCMPN-SAF algorithm (10) as

$$\boldsymbol{w}(k+1) = \boldsymbol{w}(k)+\mu\frac{\sum_{i=0}^{N-1}\alpha_i(k)\boldsymbol{u}_i(k)\mathrm{sign}(e_{i,D}(k))}{\sqrt{\sum_{i=0}^{N-1}\boldsymbol{u}_i^{\mathrm{T}}(k)\boldsymbol{u}_i(k)+\gamma}}. \tag{18}$$

Remark 1 If we consider in (18) $\alpha_i(k)=1$, for $i=0,1,\cdots,N-1$, we will have the SSAF algorithm in [8].

4. Convergence analysis

We can see that $\alpha_i(k)$ in (17) is a function of the $e_{i,D}(k)$. Therefore, we can write (18) as

$$\boldsymbol{w}(k+1) = \boldsymbol{w}(k)+\mu\frac{\sum_{i=0}^{N-1}\boldsymbol{u}_i(k)f(e_{i,D}(k))e_{i,D}(k)}{\sqrt{\sum_{i=0}^{N-1}\boldsymbol{u}_i^{\mathrm{T}}(k)\boldsymbol{u}_i(k)}} \tag{19}$$

where $f(e_{i,D}(k)) = \alpha_i(k)/|e_{i,D}(k)|$ is a nonlinear function of the subband error signal $e_{i,D}(k)$. By defining $\boldsymbol{\psi}(k) = \boldsymbol{w}_{\mathrm{o}} - \boldsymbol{w}(k)$, we have

$$\boldsymbol{\psi}(k+1) = \boldsymbol{\psi}(k)-\mu\frac{\sum_{i=0}^{N-1}\boldsymbol{u}_i(k)f(e_{i,D}(k))e_{i,D}(k)}{\sqrt{\sum_{i=0}^{N-1}\boldsymbol{u}_i^{\mathrm{T}}(k)\boldsymbol{u}_i(k)}}. \tag{20}$$

By taking the squared L_2-norm and the expectation from both sides of (20), we have

$$m(k+1) = m(k)+\mu^2\mathrm{E}\left[\sum_{i=0}^{N-1}f^2(e_{i,D}(k))e_{i,D}^2(k)\right]- 2\mu\mathrm{E}\left[\frac{\sum_{i=0}^{N-1}f(e_{i,D}(k))e_{i,D}(k)e_{a,i}(k)}{\sqrt{\sum_{i=0}^{N-1}\boldsymbol{u}_i^{\mathrm{T}}(k)\boldsymbol{u}_i(k)}}\right] \tag{21}$$

where $m(k) \triangleq \mathrm{E}[\|\boldsymbol{\psi}(k)\|^2]$ denotes the mean square deviation (MSD) and a noise-free a priori error signal is defined as $e_{a,i}(k) = \boldsymbol{\psi}(k)\boldsymbol{u}_i(k)$. With respect to (21), a function with respect to μ is obtained as

$$d(\mu) = m(k+1)-m(k) = \mathrm{E}\left[\sum_{i=0}^{N-1}f^2(e_{i,D}(k))e_{i,D}^2(k)\right]\mu^2 - 2\mathrm{E}\left[\frac{\sum_{i=0}^{N-1}f(e_{i,D}(k))e_{i,D}(k)e_{a,i}(k)}{\sqrt{\sum_{i=0}^{N-1}\boldsymbol{u}_i^{\mathrm{T}}(k)\boldsymbol{u}_i(k)}}\right]\mu. \tag{22}$$

The proposed algorithm converges in mean square sense, if we have in (21) $d(\mu)<0$. Therefore, based on (22), a necessary mean-square convergence condition is obtained as

$$0<\mu<\frac{2\mathrm{E}\left[\dfrac{\sum_{i=0}^{N-1}f(e_{i,D}(k))e_{i,D}(k)e_{a,i}(k)}{\sqrt{\sum_{i=0}^{N-1}\boldsymbol{u}_i^{\mathrm{T}}(k)\boldsymbol{u}_i(k)}}\right]}{\mathrm{E}\left[\sum_{i=0}^{N-1}f^2(e_{i,D}(k))e_{i,D}^2(k)\right]}. \tag{23}$$

We proceed by utilizing the following assumptions:

(i) The background noise $\nu(n)$ is a zero-mean white Gaussian process with the variance σ_ν^2. The impulsive interference is generally regarded as the $\chi(n)=\omega(n)\rho(n)$ [14,15,21,22], where $\omega(n)$ is a white Gaussian process with zero-mean and variance $\sigma_\omega^2=\kappa\sigma_\nu^2$ ($\kappa\gg1$), and $\rho(n)$ is a Bernoulli distribution with the probability mass function detailed as $p\{\rho(n)=1\}=P_r$, $p\{\rho(n)=0\}=1-P_r$. Note

that P_r represents the probability of the occurrence of impulsive interference. Therefore, the additive noise $\eta(n) = \nu(n) + \chi(n)$, can be considered as a Gaussian process with the zero-mean and the variance

$$\sigma_\eta^2 = \sigma_\nu^2 + P_r\sigma_\omega^2(n) = (1+P_r\kappa)\sigma_\nu^2. \tag{24}$$

(ii) The ith decimated subband input signal is approximately white [2,7], thus we conclude $\mathrm{E}[\boldsymbol{u}_i^{\mathrm{T}}(k)\boldsymbol{u}_i(k)] \approx M\sigma_{\boldsymbol{u}_i}^2(k)$.

(iii) The ratio of the expectation of two random variables is approximately equal to the expectation of the ratio between them, i.e., $\mathrm{E}(x)/\mathrm{E}(y) \approx \mathrm{E}\{x/y\}$, which is reasonable for sufficiently long filters [30,31].

By using the above assumptions, (23) is simplified as

$$0<\mu<2\frac{\sum_{i=0}^{N-1}\mathrm{E}(f(e_{i,D}(k))e_{i,D}(k)e_{a,i}(k))}{\sqrt{M\sum_{i=0}^{N-1}\sigma_{\boldsymbol{u}_i}^2(k)}\sum_{i=0}^{N-1}\mathrm{E}\left(f^2(e_{i,D}(k))e_{i,D}^2(k)\right)}. \tag{25}$$

Using Assumption (i) and Price's theorem in [32], we have

$$\mathrm{E}(f(e_{i,D}(k))e_{i,D}(k)e_{a,i}(k)) \approx P_r\frac{\mathrm{E}(e_{i_1,D}(k)e_{a,i}(k))}{\mathrm{E}\left(e_{i_1,D}^2(k)\right)}\cdot \mathrm{E}\left(f(e_{i,D}(k))e_{i_1,D}^2(k)\right) + (1-P_r)\frac{\mathrm{E}(e_{i_2,D}(k)e_{a,i}(k))}{\mathrm{E}\left(e_{i_2,D}^2(k)\right)}\cdot \mathrm{E}\left(f(e_{i,D}(k))e_{i_2,D}^2(k)\right) \tag{26}$$

where

$$\begin{cases} e_{i_1,D}(k) = e_{a,i}(k) + \chi_i(k) \\ e_{i_2,D}(k) = e_{a,i}(k) + \nu_i(k) \end{cases} \tag{27}$$

where $\chi_i(k)$ and $\nu_i(k)$ are zero-mean Gaussian sequences with variances $\sigma_{\chi_i}^2 = \frac{1}{N}(1+\kappa)\sigma_\nu^2$ and $\sigma_{\nu_i}^2 = \frac{1}{N}\sigma_\nu^2$.

Using Assumption (iii), we can obtain

$$\begin{cases} \mathrm{E}\left(e_{i_1,D}^2(k)\right) = \mathrm{E}\left(e_{a,i}^2(k)\right) + \frac{1}{N}(1+\kappa)\sigma_\nu^2 \\ \mathrm{E}\left(e_{i_2,D}^2(k)\right) = \mathrm{E}\left(e_{a,i}^2(k)\right) + \frac{1}{N}\sigma_\nu^2 \end{cases}. \tag{28}$$

Then, we have

$$\mathrm{E}\left(e_{i,D}^2(k)\right) = P_r\mathrm{E}\left(e_{i_1,D}^2(k)\right) + (1-P_r)\mathrm{E}\left(e_{i_2,D}^2(k)\right) = \mathrm{E}\left(e_{a,i}^2(k)\right) + \frac{1}{N}(P_r\kappa+1)\sigma_\nu^2. \tag{29}$$

By definitions of $m(k)$ and $e_{a,i}(k)$ denoted in this section, we have the following equation:

$$\mathrm{E}\left(e_{a,i}^2(k)\right) = \sigma_{\boldsymbol{u}_i}^2(k)m(k). \tag{30}$$

Therefore, merging (26) to (30), we get, for $i = 0,1,\cdots,N-1$,

$$\mathrm{E}(f(e_{i,D}(k))e_{i,D}(k)e_{a,i}(k)) \approx \frac{\sigma_{\boldsymbol{u}_i}^2(k)m(k)}{\sigma_{\boldsymbol{u}_i}^2(k)m(k) + \frac{(1+P_r\kappa)\sigma_\nu^2}{N}}\cdot \mathrm{E}\left(f(e_{i,D}(k))e_{i,D}^2(k)\right). \tag{31}$$

Therefore, a mean-square convergence can be achieved by a sufficient condition as

$$0<\mu<2\frac{\sum_{i=0}^{N-1}\frac{\sigma_{\boldsymbol{u}_i}^2(k)m(k)}{\sigma_{\boldsymbol{u}_i}^2(k)m(k)+\frac{(1+P_r\kappa)\sigma_\nu^2}{N}}\mathrm{E}\left(f(e_{i,D}(k))e_{i,D}^2(k)\right)}{\sqrt{M\sum_{i=0}^{N-1}\sigma_{\boldsymbol{u}_i}^2(k)}\sum_{i=0}^{N-1}\mathrm{E}\left(f^2(e_{i,D}(k))e_{i,D}^2(k)\right)}. \tag{32}$$

5. GCMPN-SAF for sparse and block-sparse system

To further speed up the convergence rate of the GCMPN-SAF algorithm for the sparse and the block-sparse systems identification processes, three proportionate versions of the GCMPN-SAF algorithm named PGCMPN-SAF, IPGCMPN-SAF, and MPGCMPN-SAF algorithms, and two L_0-GCMPN-SAF and BS-GCMPN-SAF algorithms are developed in this section.

5.1 PGCMPN-SAF

In the proposed PGCMPN-SAF algorithm, for each subband, different step-sizes are assigned to the coefficients based on the current estimated magnitudes of them. Therefore large step-size will be assigned to the coefficient with a large current magnitude, and vice versa. With the update gains proportional to the current tap weights, very fast convergence performance is obtained [7]. Vector update for the PGCMPN-SAF algorithm is given [7] by

$$\boldsymbol{w}(k+1) = \boldsymbol{w}(k) + \mu\frac{\sum_{i=0}^{N-1}\alpha_i(k)\boldsymbol{A}(k)\boldsymbol{u}_i(k)\mathrm{sign}(e_{i,D}(k))}{\sqrt{\{\boldsymbol{A}(k)\boldsymbol{U}(k)\mathrm{sign}[\boldsymbol{e}_D(k)]\}^{\mathrm{T}}\{\boldsymbol{A}(k)\boldsymbol{U}(k)\mathrm{sign}[\boldsymbol{e}_D(k)]\}+\gamma}} \tag{33}$$

where γ is a small positive constant to avoid dividing by zero, $\boldsymbol{U}(k) = [\boldsymbol{u}_0(k),\boldsymbol{u}_1(k),\cdots,\boldsymbol{u}_{N-1}(k)]$, $\boldsymbol{e}_D(k) = [e_{0,D}(k), e_{1,D},(k),\cdots,e_{N-1,D}(k)]^{\mathrm{T}}$, and $\boldsymbol{A}(k) = \mathrm{diag}(a_0(k),a_1(k),\cdots,a_{M-1}(k))$ is a diagonal matrix whose diagonal elements are calculated as

$$a_m(k)=\frac{\beta_m(k)}{\frac{1}{M}\sum_{i=0}^{M-1}\beta_i(k)} \tag{34}$$

where

$$\beta_m(k)=\max\{\rho\max\{\delta,|w_0(k)|,\cdots,|w_{M-1}(k)|\},|w_m(k)|\} \tag{35}$$

for $0\leqslant m\leqslant M-1$. The positive constant ρ (with typical value $\rho=5/M$) prevents the very small coefficients from remaining, and the positive parameter δ (with typical value $\delta=0.01$) adjusts the coefficients updating when they are zero at initialization [7,18].

5.2 IPGCMPN-SAF

Unfortunately, when the impulse response is dispersive (non-sparse), the proportionate version of algorithms converges much slower than itself. The improved proportionate version is independent of whether or not the impulse response of the system is sparse or dispersive [7]. According to [7], the update formula for the tap-weights of the IPGCMPN-SAF algorithm can be expressed as

$$\boldsymbol{w}(k+1)=\boldsymbol{w}(k)+\frac{\mu\sum_{i=0}^{N-1}\alpha_i(k)\boldsymbol{B}(k)\boldsymbol{u}_i(k)\operatorname{sign}(e_{i,D}(k))}{\sqrt{\{\boldsymbol{B}(k)\boldsymbol{U}(k)\operatorname{sign}[\boldsymbol{e}_D(k)]\}^{\mathrm{T}}\{\boldsymbol{B}(k)\boldsymbol{U}(k)\operatorname{sign}[\boldsymbol{e}_D(k)]\}+\gamma}} \tag{36}$$

where $\boldsymbol{B}(k)=\operatorname{diag}(b_0(k),b_1(k),\cdots,b_{M-1}(k))$ is a diagonal matrix whose diagonal elements are calculated as

$$b_m(k)=\frac{1-\alpha}{2M}+(1+\alpha)\frac{|w_m(k)|}{2\|\boldsymbol{w}(k)\|_1+\gamma} \tag{37}$$

where, at each iteration, the relative weighting of the proportionate and the non-proportionate adaptation is controlled by the selection $\alpha\in[-1,1]$. The values of -0.5 or 0 are typically used for α in [7,21].

5.3 MPGCMPN-SAF

The μ-law proportionate version of algorithms shows the fast convergence during the whole adaptation process. Here, by using an objective function we can obtain the step-size control factors. Also, the condition under which the fastest overall convergence will be achieved for the steepest descent algorithm has been obtained and the equations used to calculate the optimal step-size control factors in order to satisfy that condition have been derived [7]. According to [7], the update formula for the tap-weights of the MPGCMPN-SAF algorithm can be obtained as

$$\boldsymbol{w}(k+1)=\boldsymbol{w}(k)+\frac{\mu\sum_{i=0}^{N-1}\alpha_i(k)\boldsymbol{C}(k)\boldsymbol{u}_i(k)\operatorname{sign}(e_{i,D}(k))}{\sqrt{\{\boldsymbol{C}(k)\boldsymbol{U}(k)\operatorname{sign}[\boldsymbol{e}_D(k)]\}^{\mathrm{T}}\{\boldsymbol{C}(k)\boldsymbol{U}(k)\operatorname{sign}[\boldsymbol{e}_D(k)]\}+\gamma}} \tag{38}$$

where $\boldsymbol{C}(k)=\operatorname{diag}(c_0(k),c_1(k),\cdots,c_{M-1}(k))$ is a diagonal matrix whose diagonal elements are calculated as

$$c_m(k)=\frac{\beta_m(k)}{\frac{1}{M}\sum_{i=0}^{M-1}\beta_i(k)} \tag{39}$$

where

$$\beta_m(k)=\max\{\rho\max\{\delta,T(|w_0(k)|),\cdots,T(|w_{M-1}(k)|)\},T(|w_m(k)|)\} \tag{40}$$

for $0\leqslant m\leqslant M-1$. The positive constants ρ and δ are useful as mentioned in Subsection 5.2, and

$$T(|w_m(k)|)=\ln(1+\xi|w_m(k)|) \tag{41}$$

where $\xi=1/\gamma$ [20,22].

Remark 2 If we consider $\alpha_i(k)=1$, in (33), (36) and (38) for $i=0,1,\cdots,N-1$, we will have PSSAF, IPSSAF and MPSSAF algorithms respectively in [7,18,21].

5.4 L_0-norm GCMPN-SAF (L_0-GCMPN-SAF)

By adding the L_0-norm feature, which directly determines the sparsity of a vector to the cost function (6), we develop the L_0-GCMPN-SAF algorithm in this section. This extra term can lead to finding a sparse vector that reduces the cost function. According to [19,23], the weight vector of the L_0-GCMPN-SAF algorithm is updated as

$$\boldsymbol{w}(k+1)=\boldsymbol{w}(k)+\frac{\mu\sum_{i=0}^{N-1}\alpha_i(k)\boldsymbol{u}_i(k)\operatorname{sign}(e_{i,D}(k))}{\sqrt{\sum_{i=0}^{N-1}\boldsymbol{u}_i^{\mathrm{T}}(k)\boldsymbol{u}_i(k)+\gamma}}-\frac{1}{2}\mu\lambda\nabla\|\boldsymbol{w}(k)\|_0 \tag{42}$$

where $\|\cdot\|_0$ denotes the L_0-norm of a vector that counts the number of nonzero elements of a vector, $\lambda>0$ controls the intensity of the L_0-norm term and

$$\nabla\|\boldsymbol{w}(k)\|_0\triangleq[f_\beta(w_1(k)),f_\beta(w_2(k)),\cdots,f_\beta(w_M(k))]^{\mathrm{T}} \tag{43}$$

where

$$f_\beta(w_m(k))=\begin{cases}-\beta^2w_m(k)-\beta, & -1/\beta\leqslant w_m(k)<0\\ -\beta^2w_m(k)+\beta, & 0<w_m(k)\leqslant 1/\beta\\ 0, & \text{otherwise}\end{cases} \tag{44}$$

where $\beta \in [5,20]$ shows a good performance [19,23,24].

5.5 BS-GCMPN-SAF

By adding the $L_{2,0}$-norm feature, which directly determines the block-sparsity of a vector to the cost function (6), we develop the BS-GCMPN-SAF algorithm in this section. This extra term can lead to finding a block-sparse vector that reduces the cost function. According to [24, 25], the weight vector of the BS-GCMPN-SAF algorithm is updated as

$$\boldsymbol{w}(k+1)=\boldsymbol{w}(k)+\mu\frac{\sum_{i=0}^{N-1}\alpha_i(k)\boldsymbol{u}_i(k)\mathrm{sign}(e_{i,D}(k))}{\sqrt{\sum_{i=0}^{N-1}\boldsymbol{u}_i^{\mathrm{T}}(k)\boldsymbol{u}_i(k)+\gamma}}-\frac{1}{2}\mu\lambda\nabla\|\boldsymbol{w}(k)\|_{2,0} \tag{45}$$

where $\|\cdot\|_{2,0}$ denotes the $L_{2,0}$-norm of a vector that counts the number of a cluster with p length and nonzero entries. $\lambda>0$ controls the intensity of the $L_{2,0}$-norm term and

$$\nabla\|\boldsymbol{w}(k)\|_{2,0}\triangleq[f_\beta(w_1(k)),f_\beta(w_2(k)),\cdots,f_\beta(w_M(k))]^{\mathrm{T}} \tag{46}$$

where

$$f_\beta(w_m(k))=\begin{cases}2\beta^2 w_m(k)-\dfrac{2\beta w_m(k)}{\|w_{[\lceil m/p\rceil]}(k)\|_2}, & 0<\|w_{[\lceil m/p\rceil]}(k)\|_2\leqslant 1/\beta\\ 0, \quad \text{otherwise}\end{cases} \tag{47}$$

where p denotes the group partition size , β is a positive constant and $\lceil\cdot\rceil$ denotes the ceiling function.

6. Simulation results

The performance of the proposed GCMPN-SAF algorithm in a system identification process is evaluated in this section. We use two sparse types of the measured acoustic-echo-channels as the unknown systems, which are depicted in Fig. 2, where the first type is a sparse impulse response (Fig. 2(a)), and the second type is a block-sparse impulse response (Fig. 2(b)). For all the simulations, the length of the unknown system is M=512, and the adaptive filter has the same length. The input signal is an AR(1) or an AR(2) signal, generated by filtering a white Gaussian noise using a first-order $H(z)=1/(1-0.9z^{-1})$, or a second-order system $H(z)=1/(1-0.25z^{-1}-0.65z^{-2})$, respectively. The filter bank is an extended lapped transform (ELT) [33], and the number of subbands is chosen as N=4. Also, the background noise $v(n)$ is an additive white Gaussian noise with a signal-to-background-noise ratio (SBNR) of 30 dB, which is defined as $\mathrm{SBNR}=\mathrm{E}[z^2(n)]/\sigma_v^2$, where $z(n)=\boldsymbol{u}^{\mathrm{T}}(n)\boldsymbol{w}_{\mathrm{o}}$. Also, we consider the impulsive interference $\chi(n)$, as mentioned in Assumption (i), with $\sigma_\omega^2=1\,000\,\sigma_v^2$ and $P_r=0.001$. In addition, we use the normalized mean square deviation (NMSD) in dB defined as $10\lg(\|\boldsymbol{w}(k)-\boldsymbol{w}_{\mathrm{o}}\|^2/\|\boldsymbol{w}_{\mathrm{o}}\|^2)$ to measure the performance of the algorithms. In all the simulations we choose the parameters value of the competing algorithms according to the best values in their references, in such a way that all the algorithms have the same steady-state NMSD with the maximum convergence speed in achieving such a steady-state level. All the results are averaged over 50 independent trials.

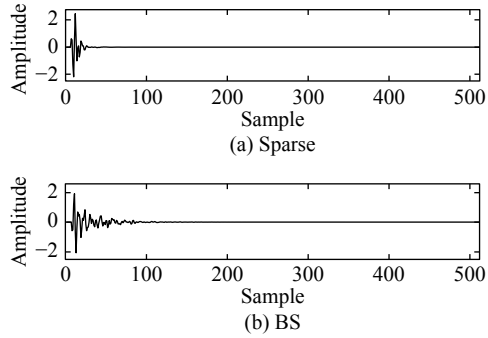

Fig. 2 Two types of measured acoustic-echo-channels as unknown systems

6.1 Choice of θ

We study the performance of the GCMPN-SAF algorithm for the different θ for block-sparse impulse response with AR(1) input signal, in presence of impulsive interference, in Fig. 3. As expected from [30], $\theta=-2$ provides the least steady-state error. Therefore, $\theta=-2$ is chosen as a proper value for the proposed algorithm in other simulations.

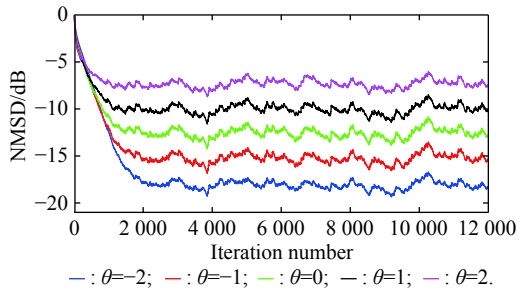

Fig. 3 NMSD learning curves of the GCMPN-SAF for different θ ($\mu=0.05$, $\rho=\delta=0.01$, $\xi=400$)

6.2 Comparisons with the versions of SSAF

Fig. 4 shows the NMSD learning curves of the robust GVSS-CMPN [30] algorithm, the non-robust algorithm with SAF structure NSAF [3] algorithm, and some robust SAF algorithms including proposed GCMPN-SAF, SSAF [8], NLSAF [13], and IWF-SSAF [16] algorithms, for the colored AR(1) and AR(2) input signals. In order to

evaluate the tracking capability of the algorithms for the AR(1) input signal in Fig. 4(a), the impulse response is selected as the sparse in Fig. 2(a) at first and abruptly is changed into the BS in Fig. 2(b) at iteration 7.5×10^3. Also the tracking capability of the algorithms for the AR(2) input signal is evaluated in Fig. 4(b) by selecting the impulse response as sparse in Fig. 2(a) at first and change it into the BS in Fig. 2(b) at iteration 3.5×10^3. The value of the parameters for Fig. 4(a) are selected as SSAF ($\mu=0.02$), NLSAF ($\mu=0.03,\alpha=1\,500$), IWF-SSAF ($\mu=0.01$), GVSS-CMPN ($\mu=0.000\,4$), NSAF ($\mu=0.5,\ 0.01$), GCMPN-SAF ($\mu=0.02$), and for Fig. 4(b) are selected as SSAF ($\mu=0.05$), NLSAF ($\mu=0.06,\alpha=1\,500$), IWF-SSA ($\mu=0.02$), GVSS-CMPN ($\mu=0.001$), NSAF ($\mu=0.5,\ 0.01$) and GCMPN-GVSS-CMPN ($\mu=0.001$), NSAF ($\mu=0.5,0.01$) and GCMPN-SAF ($\mu=0.04$). As can be seen, for both Fig. 4(a) and Fig. 4(b), the performance of the proposed algorithm is better than SSAF, NLSAF and GVSS-CMPN algorithms in terms of the convergence rate and is the best algorithm in terms of the tracking capability. As expected, the performance of the proposed algorithm is much better than the GVSS-CMPN, for the colored input signals, because it benefits from the SAF structure. It is noteworthy that although the convergence rate of the GCMPN-SAF algorithm is almost similar to the IWF-SSAF algorithm at first, but the proposed algorithm has a better tracking capability. Also, the NSAF which is not robust against impulsive interference, exhibits a poor convergence performance for both the AR(1) and the AR(2) input signals.

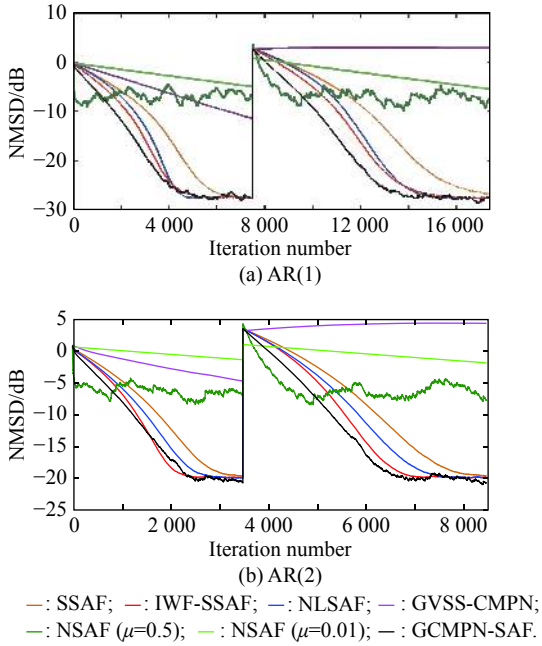

Fig. 4 NMSD learning curves of the several subband and the proposed algorithms under impulsive interference

6.3 A family of the proposed algorithm

Fig. 5 and Fig. 6 show the NMSD learning curves of the proposed algorithm and several versions of it including PGCMPN-SAF, IPGCMPN-SAF, MPGCMPN-SAF, L_0-GCMPN-SAF and BS-GCMPN-SAF algorithms for the AR(1) and the AR(2) input signals respectively. In Fig. 5(a) and Fig. 6(a), the system is sparse as Fig. 2(a) and in Fig. 5(b) and Fig. 6(b), the system is BS as Fig. 2(b). The value of the parameters are selected as GCMPN-SAF ($\mu=0.02$), PGCMPN-SAF ($\mu=0.06,\rho=\delta=0.01$), IPGCMPN-SAF ($\mu=0.05$), MPGCMPN -SAF ($\mu=0.055$, $\rho=\delta=0.01,\xi=400$), L_0-GCMPN-SAF ($\mu=0.000\,6$, $\beta=5,\lambda=0.05$) and BS-GCMPN-SAF ($\mu=0.035$, $\beta=5$, $\lambda=0.001$). As can be seen, in Fig. 5 and Fig. 6 the proportionate versions of the proposed algorithm have a better performance than their non-proportionate counterparts, GCMPN-SAF, L_0-GCMPN-SAF and BS-GCMPN-SAF. As we expect from [7], in here the MPGCMPN-SAF algorithm has a better performance than the IPGCMPN-SAF, and the IPGCMPN-SAF has a better performance than the PGCMPN-SAF. Also, the performance of the BS-GCMPN-SAF algorithm which is proposed for the block-sparse system is better than the L_0-GCMPN-SAF algorithm which is proposed for the sparse system identification, and it is more visible when the system is BS. Also it is found that expect for the colored AR(1) input signal when the system is BS (Fig. 5(b)), the L_0-GCMPN-SAF algorithm outperforms the basic GCMPN-SAF algorithm.

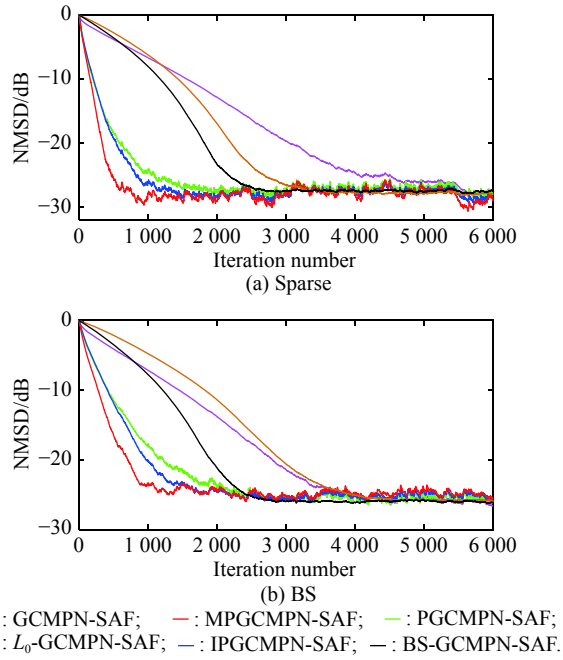

Fig. 5 NMSD learning curves of a family of the proposed algorithm with the AR(1) input signal under impulsive interference

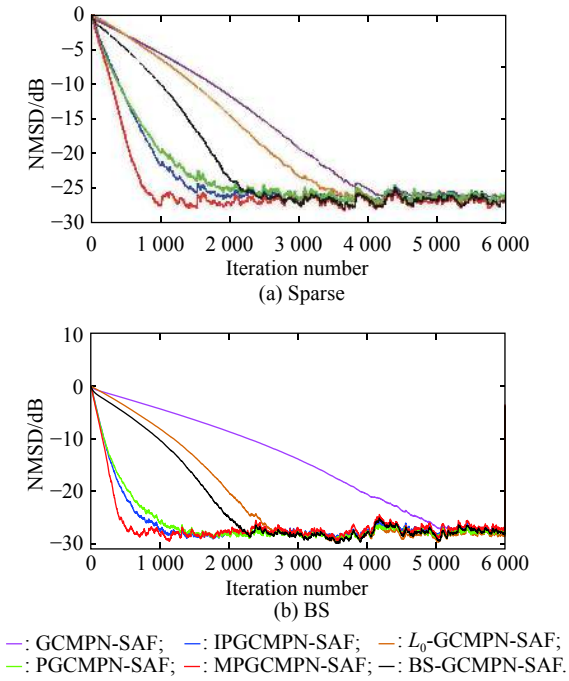

Fig. 6 NMSD learning curves of a family of the proposed algorithm with AR(2) input signal under impulsive interference

6.4 Comparisons with the other developed algorithms

Fig. 7 and Fig. 8 show the NMSD learning curves of the several developed algorithms L_0-SSAF [22], L_0-NLSAF [23], L_0-GCMPN-SAF, IPSSAF [21], IWF-IPSSAF [16], IPGCMPN-SAF and MPGCMPN-SAF, with the AR(1) and the AR(2) input signals respectively, for the sparse and the BS systems. In Fig. 7(a) and Fig. 8(a), the impulse response is sparse (Fig. 2(a)) and in Fig. 7(b) and Fig. 8(b), the impulse response is BS (Fig. 2(b)). In order to evaluate the tracking capability of the algorithms, all of the impulse responses are abruptly multiplied by −1 at iteration 5 000. The value of the parameters are selected as IPSSAF ($\mu=0.06$), L_0-SSAF ($\mu=0.000\,6$, $\gamma=0.01$, $\beta=5$), L_0-NLSAF ($\mu=0.06, \gamma=5\times10^{-4}$, $\beta=5$, $\alpha=1\,500$), IWF-IPSSAF($\mu=0.025$) and for other algorithms are selected as in Section 6.3. It is found that in Fig. 7 and Fig. 8, the proposed MPGCMPN-SAF algorithm has the best performance, and the IPGCMPN-SAF and the L_0-GCMPN-SAF algorithms have better performance than their counterparts, IPSSAF and L_0-SSAF algorithms, respectively. Although, the IWF-IPSSAF and the proposed IPGCMPN-SAF algorithms have almost the same convergence performance at first, the proposed IPGCMPN-SAF algorithm has a better tracking capability than the IWF-IPSSAF algorithm. As can be seen, the L_0-NLSAF algorithm has a better performance than the L_0-GCMPN-SAF algorithm at first, but the proposed L_0-GCMPN-SAF algorithm has a better tracking capability than the L_0-NLSAF algorithm, especially for the AR(1) input signal.

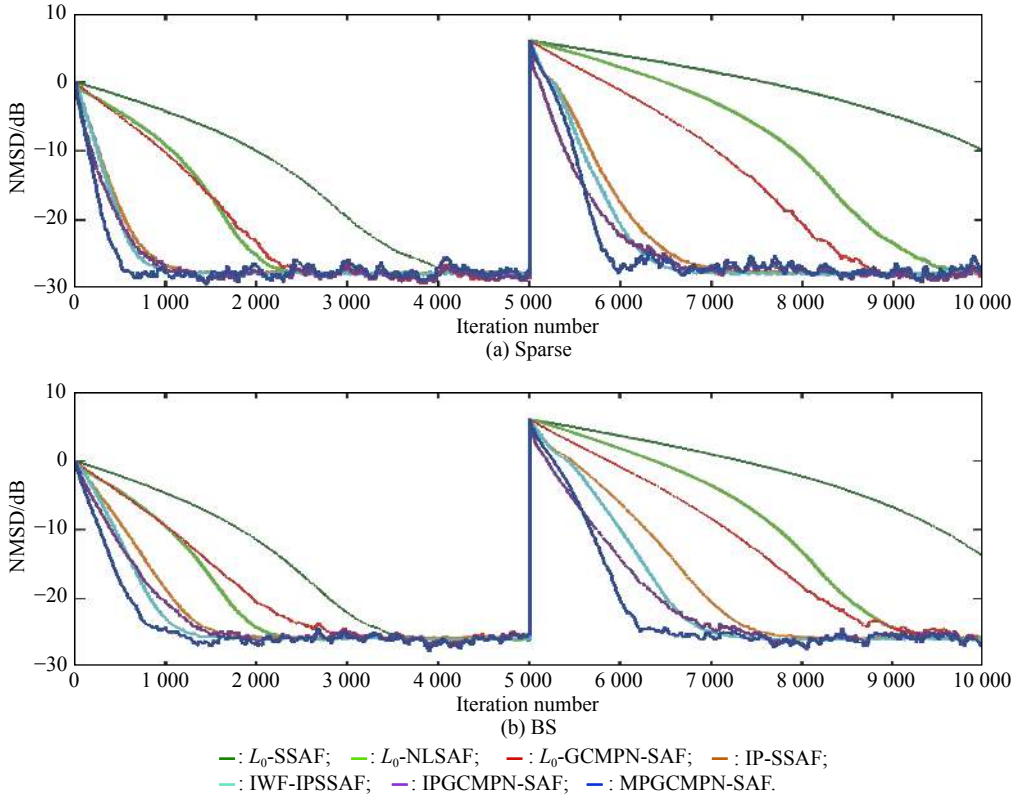

Fig. 7 NMSD learning curves of the several algorithms and the proposed algorithms for the AR(1) input signal under impulsive interference

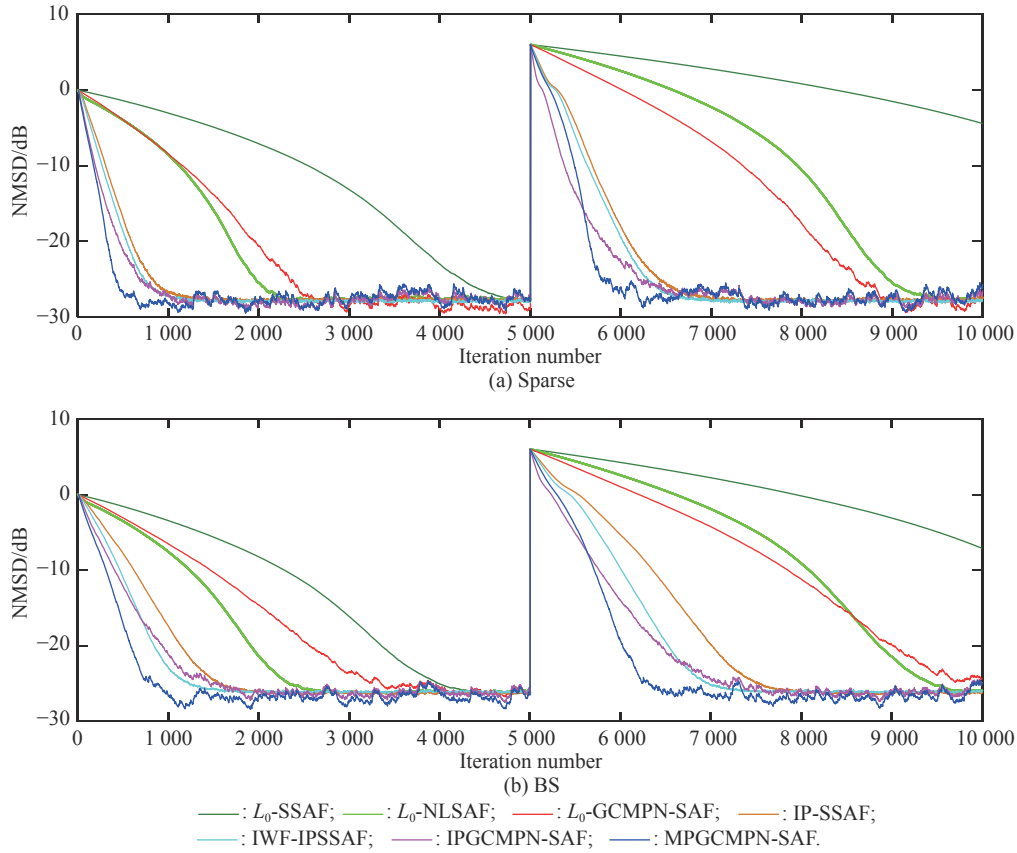

Fig. 8 NMSD learning curves of the several algorithms and the proposed algorithms for the AR(2) input signal under impulsive interference

7. Conclusions

In this paper, the new SAF algorithm named GCMPN-SAF algorithm that benefits from the GCMPN constraint in its cost function to suppress the effect of impulsive interference is proposed. Then, the convergence of the proposed algorithm is analyzed. Furthermore, in order to accelerate the convergence rate in the sparse and BS systems identification processes, several proportionate versions of the proposed algorithm PGCMPN-SAF, IP-GCMPN-SAF and MPGCMPN-SAF, L_0-GCMPN-SAF and BS-GCMPN-SAF algorithms are developed. Simulation results demonstrate that the proposed algorithms have a better performance than some other state-of-the-art algorithms in the literature with respect to the convergence rate and tracking capability.

References

[1] ALI H S. Fundamentals of adaptive filtering. New York: John Wiley & Sons, 2003.
[2] KONG A L, WOON S G, SEN M K. Subband adaptive filtering: theory and implementation. New York: John Wiley & Sons, 2009.
[3] KONG A L, WOON S G. Improving convergence of the NLMS algorithm using constrained subband updates. IEEE Signal Processing Letters, 2004, 11(9): 736–739.
[4] WILLIAM F S. Advanced television systems for terrestrial broadcasting: some problems and some proposed solutions. Proceedings of the IEEE, 1995, 83(6): 958–981.
[5] DONALD L D. Proportionate normalized least-mean-squares adaptation in echo cancellers. IEEE Trans. on Speech and Audio Processing, 2000, 8(5): 508–518.
[6] YU Y, ZHAO H Q, CHEN B D. Set-membership improved normalized subband adaptive filter algorithms for acoustic echo cancellation. IET Signal Processing, 2017, 12(1): 42–50.
[7] MOHAMMAD S E A, SIMA K. A family of proportionate normalized subband adaptive filter algorithms. Journal of the Franklin Institute, 2011, 348(2): 212–238.
[8] NI J, LI F. Variable regularization parameter sign subband adaptive filter. Electronics Letters, 2010, 46(24): 1605–1607.
[9] SHEN Z J, YU Y, HUANG T M. Two novel arctangent normalized subband adaptive filter algorithms against impulsive interferences. Circuits, Systems, and Signal Processing, 2018, 37(2): 883–900.
[10] YU Y, ZHAO H Q, CHEN B D, et al. Two improved normalized subband adaptive filter algorithms with good robustness against impulsive interferences. Circuits, Systems, and Signal Processing, 2016, 35(12): 4607–4619.
[11] SHIN J W, YOO J W, PARK P G. Variable step-size sign subband adaptive filter. IEEE Signal Processing Letters, 2013, 20(2): 173–176.
[12] WEN P W, ZHANG J S. Robust variable step-size sign subband adaptive filter algorithm against impulsive interferences. Signal Processing, 2017, 139: 110–115.
[13] SHI L, ZHAO H Q. An improved variable regularization parameter for sign subband adaptive filter. Circuits, Systems,

and Signal Processing, 2019, 38: 1396–1411.
[14] KIM J H, CHANG J H, NAM S W. Sign subband adaptive filter with l_1-norm minimization-based variable step-size. Electronics Letters, 2013, 49(21): 1325–1326.
[15] LIU Q Q, ZHAO H Q. Robust novel affine projection sign subband adaptive filter algorithm. Circuits, Systems, and Signal Processing, 2019, 38: 4141–4161.
[16] YU Y, ZHAO H Q. Novel sign subband adaptive filter algorithms with individual weighting factors. Signal Processing, 2016, 122: 14–23.
[17] WEN P W, ZHANG S, ZHANG J S. A novel subband adaptive filter algorithm against impulsive interferences and its performance analysis. Signal Processing, 2016, 127: 282–287.
[18] YU Y, ZHAO H Q. Proportionate NSAF algorithms with sparseness-measured for acoustic echo cancellation. AEU-International Journal of Electronics and Communications, 2017, 75: 53–62.
[19] YU Y, ZHAO H Q, CHEN B D. Sparse normalized subband adaptive filter algorithm with l_0-norm constraint. Journal of the Franklin Institute, 2016, 353(18): 5121–5136.
[20] CHOI Y S. Subband adaptive filtering with l_1-norm constraint for sparse system identification. Mathematical Problems in Engineering, 2013, 2013: 601623.
[21] NI J G, CHEN X P, YANG J. Two variants of the sign subband adaptive filter with improved convergence speed. Signal Processing, 2014, 96: 325–331.
[22] CHOI Y S. A new subband adaptive filtering algorithm for sparse system identification with impulsive interferences. Journal of Applied Mathematics, 2014, 2014: 704231.
[23] SHEN Z J, HUANG T M, ZHOU K. L_0-norm constraint normalized logarithmic subband adaptive filter algorithm. Signal, Image and Video Processing, 2018, 12(5): 861–868.
[24] JIANG S Y, GU Y T. Block-sparsity-induced adaptive filter for multi-clustering system identification. IEEE Trans. on Signal Processing, 2015, 63(20): 5318–5330.
[25] YAN Z H, YANG F R, YANG J. Block sparse reweighted zero-attracting normalized least mean square algorithm for system identification. Electronics Letters, 2017, 53(14): 899–900.
[26] LIU J M, GRANT S L. Proportionate adaptive filtering for block-sparse system identification. IEEE/ACM Trans. on Audio, Speech, and Language Processing, 2016, 24(4): 623–627.
[27] WANG W Y, ZHAO H Q. Block-sparse non-uniform norm constraint normalized subband adaptive filter. IET Signal Processing, 2018, 13(1): 96–102.
[28] WEI Y, ZHANG Y G, WANG C C. Block-sparsity-aware LMS algorithm for network echo cancellation. Electronics Letters, 2018, 54(15): 951–953.
[29] ZAYYANI H. Continuous mixed p-norm adaptive algorithm for system identification. IEEE Signal Processing Letters, 2014, 21(9): 1108–1110.
[30] SHI L, ZHAO H Q, AKHAROV Y. Generalized variable step size continuous mixed p-norm adaptive filtering algorithm. IEEE Trans. on Circuits and Systems II: Express Briefs, 2018, 66(6): 1078–1082.
[31] LEE H S, YIM S H, SONG W J. z^2-proportionate diffusion LMS algorithm with mean square performance analysis. Signal Processing, 2017, 131: 154–160.
[32] PRICE R. A useful theorem for nonlinear devices having Gaussian inputs. IRE Trans. on Information Theory, 1958, 4(2): 69–72.
[33] MALVAR H S. Signal processing with lapped transforms. Norwood: Artech House, 1992.

Biographies

ZAHRA Habibi was born in 1984. She received her B.S. degree from Amirkabir University of Technology, Theran, Iran, in 2007 and M.S. degree from Malek Ashtar University of Technology, Tehran, Iran, in 2011. She is currently pursuing her Ph.D. degree with the Reserch Institute for Information and Communications Technologies, Academic Center for Education, Culture and Research, Tehran, Iran. Her research interests include adaptive filters, and sparse systems identification.
E-mail: zhabibi9819@gmail.com

HADI Zayyani was born in 1978. He received his B.S., M.S., and Ph.D. degrees from Sharif University of Technology, Tehran, Iran. He is currently an assistant professor with the Department of Electrical and Computer Engineering, Qom University of Technology, Qom, Iran. His research interests include statistical signal processing, sparse signal processing, compressed sensing, adaptive filters and their applications.
E-mail: zayyani2009@gmail.com

MOHAMMAD Shams Esfand Abadi was born in 1978. He received his B.S. degree from Mazandaran University, Mazandaran, Iran, M.S. degree from Tarbiat Modares University, Tehran, Iran, and Ph.D. degree from Tarbiat Modares University, Tehran, Iran 2000, 2002 and 2007, respectively. Since 2004 he has been with the Faculty of Electrical and Computer Engineering, Shahid Rajaee Teacher Training University, Tehran, Iran. His research interests include digital filter theory and adaptive signal processing algorithms.
E-mail: mshams@sru.ac.ir